

## *Retraction*

# **Retracted: Edge Location Method for Multidimensional Image Based on Edge Symmetry Algorithm**

### **Security and Communication Networks**

Received 5 December 2023; Accepted 5 December 2023; Published 6 December 2023

Copyright © 2023 Security and Communication Networks. This is an open access article distributed under the Creative Commons Attribution License, which permits unrestricted use, distribution, and reproduction in any medium, provided the original work is properly cited.

This article has been retracted by Hindawi, as publisher, following an investigation undertaken by the publisher [1]. This investigation has uncovered evidence of systematic manipulation of the publication and peer-review process. We cannot, therefore, vouch for the reliability or integrity of this article.

Please note that this notice is intended solely to alert readers that the peer-review process of this article has been compromised.

Wiley and Hindawi regret that the usual quality checks did not identify these issues before publication and have since put additional measures in place to safeguard research integrity.

We wish to credit our Research Integrity and Research Publishing teams and anonymous and named external researchers and research integrity experts for contributing to this investigation.

The corresponding author, as the representative of all authors, has been given the opportunity to register their agreement or disagreement to this retraction. We have kept a record of any response received.

### **References**

- [1] C. Li, "Edge Location Method for Multidimensional Image Based on Edge Symmetry Algorithm," *Security and Communication Networks*, vol. 2021, Article ID 1326357, 11 pages, 2021.

## Research Article

# Edge Location Method for Multidimensional Image Based on Edge Symmetry Algorithm

Chen Li 

College of Geophysics and Petroleum Resource, Yangtze University, Wuhan 430223, China

Correspondence should be addressed to Chen Li; [lichen\\_me@163.com](mailto:lichen_me@163.com)

Received 26 June 2021; Revised 20 August 2021; Accepted 31 August 2021; Published 15 September 2021

Academic Editor: Chinmay Chakraborty

Copyright © 2021 Chen Li. This is an open access article distributed under the Creative Commons Attribution License, which permits unrestricted use, distribution, and reproduction in any medium, provided the original work is properly cited.

The most basic feature of an image is edge, which is the junction of one attribute area and another attribute area in the image. It is the most uncertain place in the image and the place where the image information is most concentrated. The edge of an image contains rich information. So, the edge location plays an important role in image processing, and its positioning method directly affects the image effect. In order to further improve the accuracy of edge location for multidimensional image, an edge location method for multidimensional image based on edge symmetry is proposed. The method first detects and counts the edges of multidimensional image, sets the region of interest, preprocesses the image with the Gauss filter, detects the vertical edges of the filtered image, and superposes the vertical gradient values of each pixel in the vertical direction to obtain candidate image regions. The symmetry axis position of the candidate image region is analyzed, and its symmetry intensity is measured. Then, the symmetry of vertical gradient projection in the candidate image region is analyzed to verify whether the candidate region is a real edge region. The multidimensional pulse coupled neural network (PCNN) model is used to synthesize the real edge region after edge symmetry processing, and the result of edge location of the multidimensional image is obtained. The results show that the method has strong antinoise ability, clear edge contour, and precise location.

## 1. Introduction

The most basic feature of an image is edge, which is the junction of one attribute area and another attribute area in the image. It is the place where the regional attributes mutate. It is the most uncertain place in the image and the place where the image information is most concentrated. The edge of an image contains rich information. Edge widely exists between objects and background, objects and objects, and primitives and primitives, so it is an important feature of image segmentation [1]. There are three kinds of common image edges. The first one is step edge, which is from one gray level to another gray level much higher than it. The second one is roof edge, which gradually increases to a certain degree and then decreases. Another is line edge, whose gray level changes from one level to another and then returns. Edge location is one of the most basic contents in image processing and recognition. An image is an information system, and a lot of information is provided by its

contour edge. Therefore, edge location plays an important role in image processing, and its positioning method directly affects the image effect [2]. Multidimensional images are not susceptible to external environmental impact and have more feature information. The recognition accuracy is not affected by single feature change, and it has natural symmetry [3]. Symmetry is a common feature of many natural objects and artificial phenomena. It is widely used in image processing to describe the shape features of objects. Symmetry detection plays an important role in object recognition and location, multidimensional object reconstruction, and other fields [4].

Image edge location methods mainly include the spatial moment location method and the subpixel location method, each of which has its own advantages and disadvantages. Spatial moment location is a common method in a fixed background. It can generally provide complete edge data, but its location effect depends on the merits of background model updating algorithm. It is particularly sensitive to scene changes, such as illumination and interference from

external unrelated events [5]. The subpixel location method has strong adaptability to scene changes, but, generally, it cannot locate all the relevant edge pixels completely. It produces holes in the image entity, and it is easy to miss the location of some image edges [6]. In view of the shortcomings of the above two methods, this paper proposes an edge location method for the multidimensional image based on edge symmetry algorithm to improve the accuracy of edge location for the multidimensional image. This model was defined and tested for pictures in order to assess the performance of the suggested model. One of the test parameters was the number of iterations. The result is evaluated using the Pratt quality factor value. The suggested model's output is compared to the performance of the two approaches described above.

## 2. Edge Symmetry Algorithm for Locating Multidimensional Image's Edges

**2.1. Edge Detection and Statistics.** Firstly, the image is preprocessed to improve the image quality; secondly, the edge gradient in the edge region of the multidimensional image is calculated by using the vertical direction of the Sobel operator [7]; then, the candidate region is determined according to the characteristics of large jump and the large number of edge changes between the edge and the background.

### 2.1.1. Image Preprocessing

- (1) Region of interest: in order to simultaneously detect a large range of image regions and reduce the computational complexity, the algorithm sets multiple regions of interest according to the number of pixels occupied by the image. The resolution of the image is  $720 \times 288$ , and a region of interest with a size of  $200 \times 50$  is set in the three regions at the bottom of the image.
- (2) Image preprocessing: in order to improve the accuracy of location, the image in the region of interest is preprocessed [8]. The color image is transformed into the gray image, and the noise is filtered by Gauss smoothing. The Gauss filter is a kind of linear smoothing filter which chooses weights according to the shape of Gauss function (i.e., normal distribution function). Gauss smoothing filter is very effective for removing noise which obeys normal distribution.

One-dimensional zero-mean Gauss function is

$$g_{(x)} = e^{-(x^2/2\sigma^2)}, \quad (1)$$

where the Gaussian distribution parameter  $\sigma$  determines the width of the Gaussian filter. For image edge processing, two-dimensional zero-mean discrete Gauss function is often used as the smoothing filter:

$$G(x, y) = Ae^{-(x^2+y^2/2\sigma^2)} = Ae^{-(r^2/2\sigma^2)}. \quad (2)$$

Sampling and quantifying the continuous Gauss distribution above and normalizing the template, the discrete template is obtained:

$$G^3 = \frac{1}{16} \begin{pmatrix} 1 & 2 & 1 \\ 2 & 4 & 2 \\ 1 & 2 & 1 \end{pmatrix}. \quad (3)$$

The Gauss filter can solve the problem of spatial distance weighting and pixel gradient. The pixel gradient reflects the image edge characteristics, which is very helpful for edge location of the multidimensional image.

**2.1.2. Vertical Edge Detection.** Vertical edge detection is applied to the preprocessed image. The essence of edge detection is to find the fast-changing region of brightness in the image, that is, the region whose first derivative of brightness is larger in magnitude than the specified range value. Because the vertical edge of the image has the strongest symmetry, in order to eliminate interference and reduce the amount of calculation, the proposed algorithm only processes the vertical component of the edge [9]. The vertical mask of the Sobel operator is used to digitally approximate the first derivative; that is, the vertical gradient of the image is calculated by formula (1) and presented as

$$G(x, y) = |(f(x+1, y-1) + 2f(x+1, y) + f(x+1, y+1)) - (f(x-1, y-1) + 2f(x-1, y) + f(x-1, y+1))|, \quad (4)$$

where  $f(x, y)$  is the gray value of the pixel  $(x, y)$  and  $G(x, y)$  is the approximate first derivative of the point in the vertical direction, i.e., the vertical gradient value.

**2.1.3. Gradient Statistics.** The vertical gradient values of each pixel are projected in the vertical direction:

$$B(i) = \sum_{j=0}^{H-1} G(i, j), \quad (5)$$

where  $H$  is the height of the detection block,  $B$  is the vertical superposition projection of the detection block, and  $i$  is the column position of the vertical superposition projection.

The average value of vertical gradient projection is

$$\bar{B} = \sum_{i=0}^{W-1} \frac{B(i)}{W}, \quad (6)$$

where  $W$  is the width of the region of interest and  $B$  is the mean value.

The mean value of vertical gradient projection is greater due to the large leap between edge and background, the significant number of edge modifications, and the quantity of vertical edges. In addition, the edge of the image is not susceptible to external environmental impact. Shadows, lights, and other interference factors cannot form a strong vertical gradient value, which will not have a great impact on

the accuracy of location [10]. Therefore, when the mean value of vertical gradient projection exceeds a certain threshold, it can be determined as a candidate image region.

**2.2. Symmetry Analysis.** After edge identification and statistics, the symmetry of potential picture areas is examined. The image's symmetry axis direction has been established as the vertical direction. It is required to establish the symmetrical axis's position and quantify its symmetrical intensity [11]. The symmetry of the candidate image region's vertical gradient projection is examined to determine whether the candidate region is a true edge region.

**2.2.1. Symmetry Analysis.** The gradient vertical projection value obtained in the previous section is regarded as one-dimensional function  $g(x)$ , assuming that its symmetric axis coordinate is  $X_s (W/2 \leq X_s \leq W - W/2)$  and  $W$  is the width of the symmetric region, which can be selected according to the width of the image [8]. Let  $u = X - X_s$ ;  $g(u)$  is a function with  $X_s$  as the origin of the coordinate. Since an arbitrary function  $f(x)$  can be expressed as the sum of an odd function and an even function, as mentioned in formula (7), the odd function component and even function component of the definable function  $g(x) = g(X_s + u)$  are, respectively,

$$\begin{cases} O(u, X_s) = \frac{g(X_s + u) - g(X_s - u)}{2}, \\ E(u, X_s) = \frac{g(X_s + u) + g(X_s - u)}{2}, \\ -W/2 \leq u \leq W/2. \end{cases} \quad (7)$$

The even function components are normalized to make the mean value as 0 by using

$$E_n(u, X_s) = E(u, X_s) - \frac{1}{W} \int_{-w/2}^{+w/2} E(u, X_s) du. \quad (8)$$

Then, the symmetry is measured by comparing the energy of odd component function with that of an even component function:

$$S(X_s) = \frac{\int_{-w/2}^{+w/2} E_n(u, X_s)^2 du - \int_{-w/2}^{+w/2} O(u, X_s)^2 du}{\int_{-w/2}^{+w/2} E_n(u, X_s)^2 du + \int_{-w/2}^{+w/2} O(u, X_s)^2 du}, \quad (9)$$

$$-1 \leq S(X_s) \leq 1,$$

where  $S = 1$ , and it is completely symmetric, and when  $S = -1$ , it is completely asymmetric.

**2.2.2. Verification of Candidate Region.** According to the size of the candidate region, the symmetric axis is searched by changing the  $X_s$  value of the symmetric coordinate axis in a certain range. In the search interval,  $X_s$  is taken as the coordinate of the symmetrical axis of the candidate region when the maximum value of the symmetrical evaluation

function  $S(X_s)$  appears. When  $S(X_s) > 0.5$  is located on the symmetrical axis, it is considered to be in line with the candidate region.

In addition, the vertical projection value of the edge should be the largest on both sides of the image edge, so locating the maximum value on both sides of the symmetric axis of the even function component  $E(u, X_s)$  can determine the approximate left and right boundaries of the image edge. Since the edge width of image satisfies certain constraints [12–15], it can be further verified whether it is a real image edge.

**2.3. PCNN Edge Location of Multidimensional Image.** The real edge region processed by edge symmetry is synthesized by PCNN for edge location. The PCNN model plays an important role in image denoising, smoothing, segmentation, edge extraction, and feature extraction. As multidimensional images provide richer target information than two-dimensional images, the edge location of the multidimensional image has attracted more and more attention [16–19]. At present, PCNN can only deal with two-dimensional images directly, which have great limitations. This paper introduces vector matrix and multidimensional convolution ( $\otimes$ ) to extend PCNN, which is called the multidimensional PCNN model for short, and the application of PCNN is extended so that PCNN can directly realize multidimensional image's edge location [20–23].

Figure 1(a) represents the process of two-dimensional PCNN, and Figure 1(b) represents the multidimensional PCNN. It can be seen from Figure 1 that a multidimensional PCNN is equivalent to the edge location of PCNN image with three real edge regions. The multidimensional PCNN model satisfies the following formulas:

$$F_{ij}[n] = s_{ij}, \quad (10)$$

$$L_{ij}[n] = Y_{ij}[n-1] \otimes W, \quad (11)$$

$$U_{ij}[n] = F_{ij}[n-1](1 + \beta L_{ij}[n]), \quad (12)$$

$$Y_{ij}[n] = \begin{cases} 1, & U_{ij}[n] > E_{ij}[n], \\ 0, & \text{other,} \end{cases} \quad (13)$$

$$E_{ij}[n] = \exp(-\alpha_E) E_{ij}[n-1] + \nu_E Y_{ij}[n-1], \quad (14)$$

where  $S$ ,  $F$ ,  $L$ ,  $U$ ,  $Y$ , and  $W$  are vector matrices,  $s_{ij}$  is the external input stimulus signal (here is the gradient vector  $(G_{ij}^a, G_{ij}^b, G_{ij}^c)$ ) of the input image at  $(i, j)$ ,  $F_{ij}[n]$  is the  $n$ th feedback input of the  $(i, j)$ th image,  $L_{ij}[n]$  is the  $n$ th connection input of the  $(i, j)$ th image,  $U_{ij}[n]$  is the internal active item of the image,  $E_{ij}$  is the dynamic threshold,  $Y_{ij}$  is the output sequence of PCNN,  $W$  is the intensity constant of adjacent connected images in the connection domain,  $\nu_E$  is the intrinsic potential in  $E_{ij}[n]$ ,  $\alpha_E$  is the attenuation time constant of  $E_{ij}[n]$ ,  $n$  is the iteration number, which can be selected according to actual needs, and  $\otimes$  is the multidimensional convolution; if convolution is the multidimensional convolution and conv2 is the two-dimensional

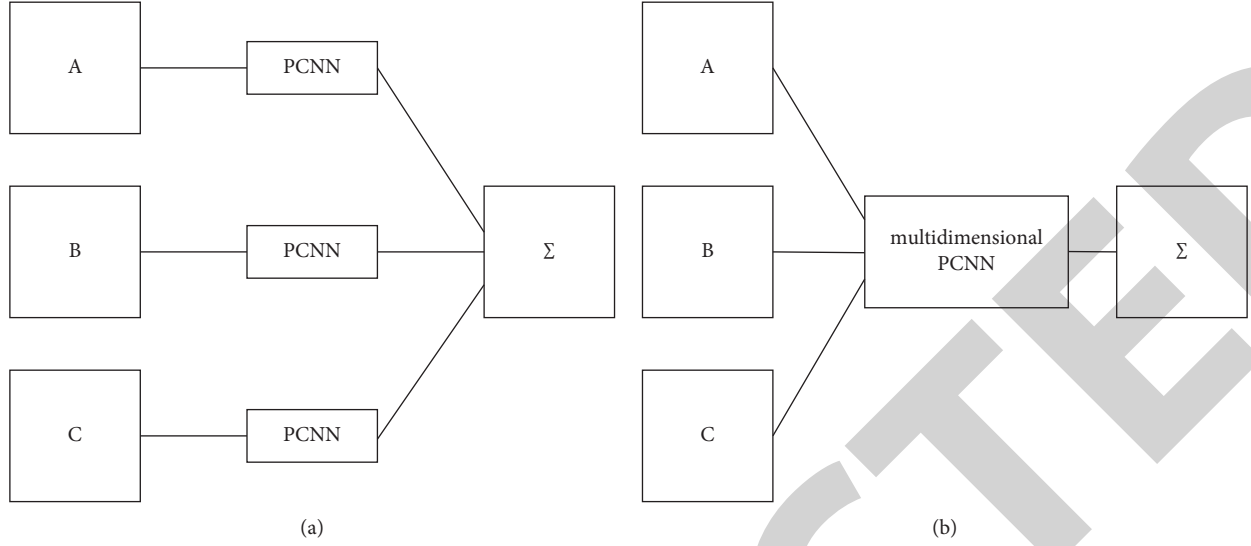


FIGURE 1: (a) Two-dimensional and (b) multidimensional PCNN processing process.

convolution, then  $Y_{conv} = (Y_A \text{conv} 2W_A, Y_B \text{conv} 2W_B, Y_C \text{conv} 2W_C)$ .

According to the principle of vector gradient and the definition of multidimensional PCNN, we can design an edge location algorithm for the multidimensional image based on the real-edge region obtained from edge symmetry. The flowchart of the algorithm is shown in Figure 2.

- (1) Vector gradient operator DV is used to compute the gradient of the real-edge region processed by the symmetry of the input edge, which reflects the change of color information in the neighborhood of the pixel and provides the basis for PCNN edge location [24, 25].
- (2) Initialization of PNCC:  $E_{ij}$  is the maximum value in gradient graph, which can suppress the ignition of small gradient pixels, and only large gradient can ignite.  $Y_{ij}$  is all zero.
- (3) The vector gradient obtained in step 1 is input into the multidimensional PNCC model, and the threshold  $E_{ij}$  is attenuated to determine whether the value of the internal activity item is greater than the threshold value. If the value is greater than the threshold value,  $Y$  is set to 1, otherwise 0 is set.
- (4) If the number of iterations is less than the prescribed maximum number of iterations, all the pixels will return to step 3 to continue iteration after judging, otherwise the iteration will end [26–28].
- (5) Finally, the best processing effect is selected from the real edge regions and obtained when the number of iterations is small, and the final multidimensional image's edges are obtained by adding the three channel results of the multidimensional PCNN model. Since the threshold is attenuated from the maximum gradient value, when the iteration times are small, the small gradient is suppressed [29]. Only those large gradient values will ignite first, the sharp

change of pixel points, namely, edge points, can be detected.

Because the convolution in formula (11) is multidimensional convolution and PCNN is vector operation, there is no need for three channels to run separately. Parallel operation reduces the operation time. Finally, the edge subgraphs of three channels are added together to obtain the final edge location results. The location results are determined by the output of all channels, which can locate the edges of multidimensional images more accurately.

### 3. Results

In order to verify the accuracy of edge location for multidimensional images, the proposed method is compared with the subpixel method and the spatial distance method.

The Pratt quality factor is a representative objective evaluation index of edge detection results and a more comprehensive evaluation parameter. Therefore, the Pratt quality factor is selected to objectively evaluate the performance of image's edge location of different edge location methods. At the same time, the vertical standard map is used to test. Noise and signal-to-noise ratio are added to analyze different methods under different iterations. The result of edge location of the multidimensional image is shown in Figures 3 and 4.

Figure 3 represents the variation of quality factor with respect to the signal-to-noise ratio (SNR) for single iteration, i.e.,  $N = 1$ . The results show that the Pratt quality factor value of the proposed method is higher than that of the other two methods. It is clear from Figure 3 that the edge location effect of the proposed method is better than that of the other two methods, but the effect is not obvious.

Figure 4 represents the Pratt quality factor vs. signal-to-noise ratio (SNR) for three number of iterations, i.e.,  $N = 3$ . The Pratt quality factor for the proposed method is superior to the other two methods. The infrared image House and

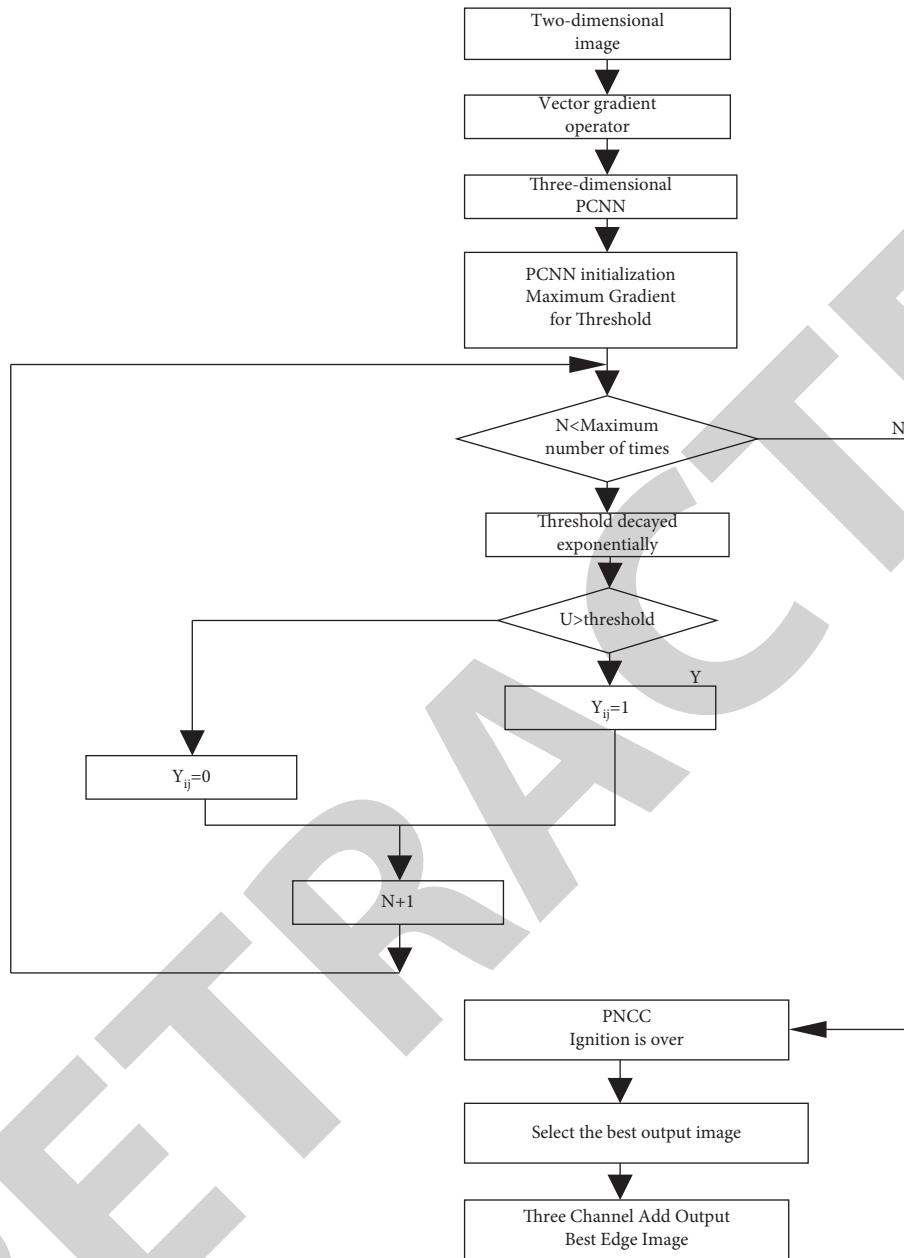


FIGURE 2: Algorithm flowchart.

Lena are selected to simulate and compare the proposed method with the subpixel method and the space distance method. The simulation results are shown as follows.

As can be seen in Figures 5–14, the image edge image localized by the proposed method is better than the image edge localized by the nonenhanced edge image, the subpixel method, and the spatial moment method. The image processed by the proposed method not only has clearer layers between regions but also enhances the gray contrast on both sides of the edge. The simulation results also show that the edge location of this method is more precise.

In order to verify the edge location effect of this method in multidimensional images, two multiband remote-sensing images are selected for edge location, and the location results

are shown in the figures. Figure 15 is the IKONOS satellite image, with the size of  $544 \times 342$ , and membership function parameters of  $a = 23$ ,  $b = 159$ , and  $T = 0.85$ . Figure 16 is the IKONOS pseudocolor remote-sensing image, with the size of  $600 \times 450$ , and membership function parameters of  $a = 11$ ,  $b = 173$ , and  $T = 0.79$ . The subpixel method, the spatial moment method, and the proposed method describe the results of edge location in Figure 15, by using Figures 17–19. The subpixel method, the spatial moment method, and the proposed method describe the results of edge location in Figure 16, by using Figures 20–22.

According to the above figures, we can see that the multidimensional image’s edges located by the subpixel method and the spatial moment method contain many false

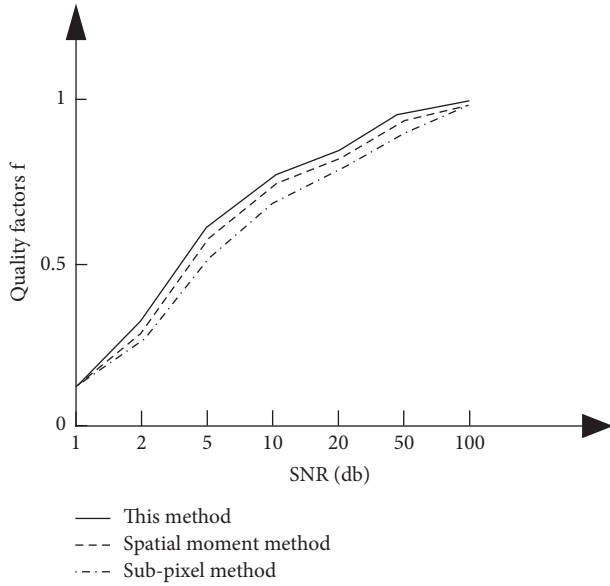
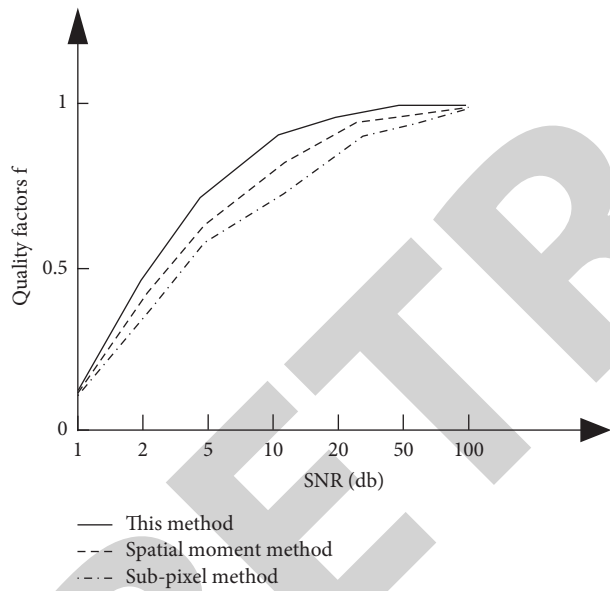
FIGURE 3: Evaluation results,  $N=1$ .FIGURE 4: Evaluation results,  $N=3$ .

FIGURE 5: House original.

FIGURE 6: Edge diagram without enhancement ( $N=0$ ).

FIGURE 7: The method edge location graph in this paper.



FIGURE 8: Subpixel method edge map.

edges and secondary edges, and the effect is not ideal. However, the method in this paper is accurate and effective in multidimensional image's edge location.

In order to verify the location accuracy of the proposed method, the test image is selected as the multidimensional image of the microgear scanned by the multidimensional profiler. Considering the smoothing effect of the actual optical system and sensors on the image, the multidimensional image of the microgear is smoothed by  $3 \times 3$  pixel



FIGURE 9: Spatial moment method edge location map.



FIGURE 12: The method edge location diagram in this paper.



FIGURE 10: Original map of Lena.



FIGURE 13: Subpixel method edge map.



FIGURE 11: Edge diagram without enhancement ( $N=0$ ).



FIGURE 14: Spatial moment method edge mapping.

neighborhood filter, and then, the standard multidimensional test image for experiment is generated. Multidimensional profilometer is a precision-measuring instrument. Its dimension measuring accuracy can reach the level of nm. In this paper, the measured data are taken as actual data. Tables 1–3 are the results of edge location of multidimensional image of microgears by three methods in simulation experiments.

By comparing and analyzing Tables 1–3, the average error of the proposed method is  $2.4 \mu\text{m}$  when locating the multidimensional image edge of the microgear, while the average error of the subpixel method and the spatial moment method is  $18.2 \mu\text{m}$  and  $13.4 \mu\text{m}$  when locating the multidimensional image edge. Compared with the subpixel method and the spatial moment method, the proposed method is more accurate than the subpixel method and the

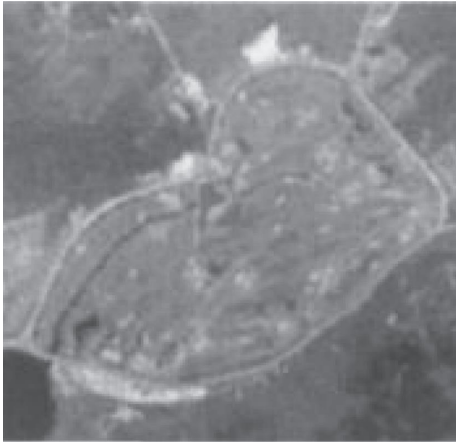


FIGURE 15: Original image of IKONOS satellite image.



FIGURE 18: Spatial moment method edge positioning.

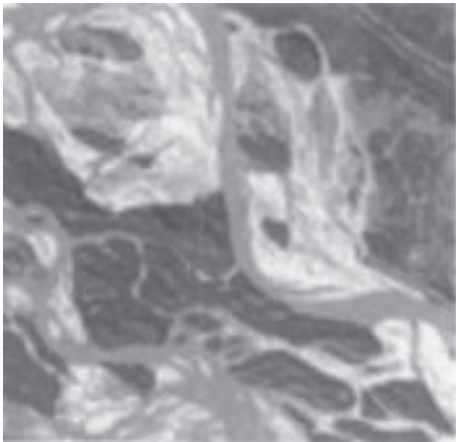


FIGURE 16: Original image of IKONOS false color remote-sensing images.

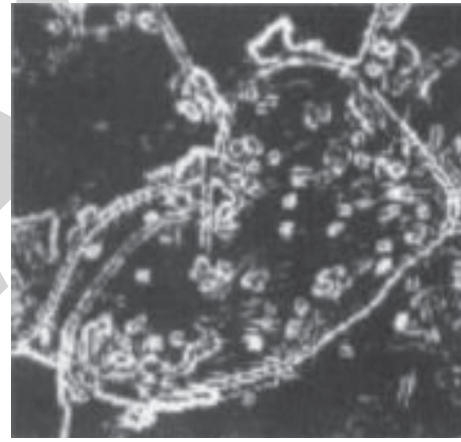


FIGURE 19: Edge positioning of this method.



FIGURE 17: Subpixel method edge positioning.

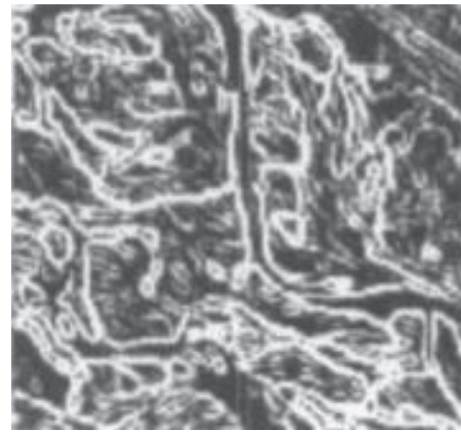


FIGURE 20: Subpixel method edge positioning.



FIGURE 21: Spatial moment method edge positioning.



FIGURE 22: Edge positioning of this method.

TABLE 1: The method of edge positioning of the multidimensional image of the microgear.

Label point	Actual distance ( $\mu\text{m}$ )	This method distance ( $\mu\text{m}$ )	Error against actual value ( $\mu\text{m}$ )
D1	749	750	1
D2	752	750	2
D3	741	745	4
D4	771	773	2
D5	761	765	4
D6	1954	1956	2
D7	1952	1949	3
D8	1987	1986	1
D9	1961	1964	3
D10	1974	1972	2

spatial moment method by  $15.8 \mu\text{m}$  and  $11 \mu\text{m}$ . It can be seen that the proposed method can locate the multidimensional image edge accurately.

#### 4. Discussion

In view of the above analysis and discussion, this paper proposes an edge location method for the multidimensional image based on edge symmetry, which can process the multidimensional image with strong antinoise and can

locate the multidimensional image's edge more precisely and clearly, and the effect is obvious. The analysis is from the following three aspects:

- (1) In this paper, a Gauss filter is introduced to pre-process multidimensional images. The problem of spatial distance weighting and pixel gradient is well solved by the Gauss filter. The pixel gradient reflects the image edge features, which is very helpful for multidimensional image's edge location.

TABLE 2: Subpixel method for edge positioning of microgear multidimensional image.

Label point	Actual distance ( $\mu\text{m}$ )	This method distance ( $\mu\text{m}$ )	Error against actual value ( $\mu\text{m}$ )
D1	749	733	16
D2	752	739	13
D3	741	727	14
D4	771	759	12
D5	761	746	15
D6	1954	1941	13
D7	1952	1940	12
D8	1987	1975	12
D9	1961	1946	15
D10	1974	1962	12

TABLE 3: Spatial moment method for edge positioning of microgear multidimensional image.

Label point	Actual distance ( $\mu\text{m}$ )	This method distance ( $\mu\text{m}$ )	Error against actual value ( $\mu\text{m}$ )
D1	749	767	18
D2	752	771	19
D3	741	762	21
D4	771	787	16
D5	761	779	18
D6	1954	1970	16
D7	1952	1969	17
D8	1987	2005	18
D9	1961	1980	19
D10	1974	1994	20

- (2) In this paper, we analyze the symmetric axis position of candidate image region and measure its symmetry intensity. Then, the vertical gradient projection symmetry of the candidate image region is analyzed to verify whether the candidate region is a real edge region. The symmetry analysis of the multidimensional image is carried out. The accuracy of image's edge location and robustness of the algorithm are effectively improved by means of the verification of vertical gradient projection's mean value, symmetry detection, and width constraint.
- (3) After introducing vector matrix and multidimensional convolution into PCNN, this paper generalizes PCNN, which is called the multidimensional PCNN model for short, and expands the application of PCNN so that PCNN can directly realize multidimensional image's edge location. The multidimensional PCNN model is used to synthesize the real-edge region after edge symmetry processing, and the result of edge location of the multidimensional image is obtained.

## 5. Conclusions

The proposed method uses the Gauss filter to preprocess the multidimensional image, which can not only suppress noise but also better preserve image edge and high-frequency detail information so that the edge image outline is clear, the edge position is precise, and the error is small, which is of great benefit to image location research. Moreover, the real edge region after edge symmetry processing is synthesized

by using the multidimensional PCNN model to obtain accurate edge location results of the multidimensional image. The experimental results show that the proposed method is superior to the subpixel method and the spatial distance method in terms of noise immunity and multidimensional image's location accuracy and clarity. The location accuracy of the multidimensional image of microgears by using the proposed method is  $2.4\mu\text{m}$  on an average, which is more accurate than the subpixel method and the spatial moment method with  $15.8\mu\text{m}$  and  $11\mu\text{m}$ . The results for the proposed method are superior to the conventional methods; also, as the number of iterations increases, the quality of results also increases. It can be seen that the proposed method has clear edge location and high accuracy in the multidimensional image.

## Data Availability

The data used to support the findings of this study are available from the corresponding author upon request.

## Conflicts of Interest

The author declares that there are no conflicts of interest regarding the publication of this paper.

## References

- [1] Z. Wang, Z. Tang, and X. Zhang, "Reflection symmetry detection using locally affine invariant edge correspondence," *IEEE Transactions on Image Processing*, vol. 24, no. 4, pp. 1297–1301, 2015.

- [2] Z. H. Pan, A. H. Cai, C. Q. Liu, P. Li, and W. S. Feng, "Research on a new variation model based speckle noise despeckling algorithm," *Journal of China Academy of Electronics and Information Technology*, vol. 11, pp. 376–382, 2016.
- [3] V. Bhatia, S. Kaur, K. Sharma, P. Rattan, V. Jagota, and M. A. Kemal, "Design and simulation of capacitive MEMS switch for ka band application," *Wireless Communications and Mobile Computing*, vol. 2021, Article ID 2021513, 8 pages, 2021.
- [4] C. Chakraborty, "Chronic wound image analysis by particle swarm optimization technique for tele-wound network," *Wireless Personal Communications*, vol. 96, no. 3, pp. 3655–3671, 2017.
- [5] T. Hachaj and M. R. Ogiela, "Full body movements recognition - unsupervised learning approach with heuristic R-GDL method," *Digital Signal Processing*, vol. 46, pp. 239–252, 2015.
- [6] A. Kishor, C. Chakraborty, and W. Jeberson, "Reinforcement learning for medical information processing over heterogeneous networks," *Multimedia Tools and Applications*, vol. 80, pp. 23983–24004, 2021.
- [7] M. O. Delchini, J. C. Ragusa, and R. A. Berry, "Entropy-based viscous regularization for the multi-dimensional Euler equations in low-mach and transonic flows," *Computers & Fluids*, vol. 118, pp. 225–244, 2015.
- [8] A. S. Poplavnoi, "Anisotropic sublattices in cubic perovskite and their symmetry in multidimensional crystal space," *Crystallography Reports*, vol. 61, no. 3, pp. 337–344, 2016.
- [9] R. Sengupta and P. D. Orkwis, "Proving algorithm symmetry for flows exhibiting symmetry breaking," *AIAA Journal*, vol. 34, pp. 2193–2195, 2015.
- [10] X. J. Zhang and D. Y. Fan, "Tilt license plate image edge fuzzy feature recognition method research," *Computer Simulation*, vol. 34, pp. 372–375, 2017.
- [11] X. Li, "Research on target tracking technology based on Mean-Shift algorithm," *Automation & Instrumentation*, vol. 4, pp. 20–22, 2016.
- [12] M. Craddock, "Fourier type transforms on Lie symmetry groups," *Journal of Mathematical Physics*, vol. 56, pp. 1–36, 2015.
- [13] B. Cao, J. Zhao, Y. Gu, S. Fan, and P. Yang, "Security-aware industrial wireless sensor network deployment optimization," *IEEE Transactions on Industrial Informatics*, vol. 16, no. 8, pp. 5309–5316, 2020.
- [14] B. Cao, J. Zhao, Y. Gu, Y. Ling, and X. Ma, "Applying graph-based differential grouping for multiobjective large-scale optimization," *Swarm and Evolutionary Computation*, vol. 53, Article ID 100626, 2020.
- [15] M. Chao, C. Kai, and Z. Zhiwei, "Research on tobacco foreign body detection device based on machine vision," *Transactions of the Institute of Measurement and Control*, vol. 42, 2020.
- [16] L. Liu, G. Xu, and H. Yuan, "Stability of spherically symmetric subsonic flows and transonic shocks under multidimensional perturbations," *Advances in Mathematics*, vol. 291, pp. 696–757, 2016.
- [17] A. Kishor and C. Chakraborty, "Task offloading in fog computing for using smart ant colony optimization," *Wireless Personal Communications*, 2021.
- [18] J. Liu, C. Wu, G. Wu, and X. Wang, "A novel differential search algorithm and applications for structure design," *Applied Mathematics and Computation*, vol. 268, pp. 246–269, 2015.
- [19] Q. Long, C. Wu, and X. Wang, "A system of nonsmooth equations solver based upon subgradient method," *Applied Mathematics and Computation*, vol. 251, pp. 284–299, 2015.
- [20] Mukhsar, B. Abapihi, A. Sani, E. Cahyono, P. Adam, and F. Aini Abdullah, "Extended convolution model to bayesian spatio-temporal for diagnosing the DHF endemic locations," *Journal of Interdisciplinary Mathematics*, vol. 19, no. 2, pp. 233–244, 2016.
- [21] K. Jairath, N. Singh, V. Jagota, and M. Shabaz, "Compact ultrawide band metamaterial-inspired split ring resonator structure loaded band notched antenna," *Mathematical Problems in Engineering*, vol. 2021, Article ID 5174455, 12 pages, 2021.
- [22] Z. Lv and H. Song, "Mobile internet of things under data physical fusion technology," *IEEE Internet of Things Journal*, vol. 7, no. 5, pp. 4616–4624, 2020.
- [23] C. Wu, X. Wang, M. Chen, and M. J. Kim, "Differential received signal strength based RFID positioning for construction equipment tracking," *Advanced Engineering Informatics*, vol. 42, 2019.
- [24] T. Li and W. Yang, "Solution to chance constrained programming problem in swap trailer transport organisation based on improved simulated annealing algorithm," *Applied Mathematics and Nonlinear Sciences*, vol. 5, no. 1, pp. 47–54, 2020.
- [25] C. Sharma, A. Bagga, B. K. Singh, and M. Shabaz, "A novel optimized graph-based transform watermarking technique to address security issues in real-time application," *Mathematical Problems in Engineering*, vol. 2021, Article ID 5580098, 27 pages, 2021.
- [26] G.-Q. G. Chen and M. Perepelitsa, "Vanishing viscosity solutions of the compressible euler equations with spherical symmetry and large initial data," *Communications in Mathematical Physics*, vol. 338, no. 2, pp. 771–800, 2015.
- [27] C. Zuo, J. Sun, J. Li, A. Asundi, and Q. Chen, "Wide-field high-resolution 3D microscopy with fourier ptychographic diffraction tomography," *Optics and Lasers in Engineering*, vol. 128, Article ID 106003, 2020.
- [28] C. Zuo, J. Sun, J. Li, J. Zhang, A. Asundi, and Q. Chen, "High-resolution transport-of-intensity quantitative phase microscopy with annular illumination," *Scientific Reports*, vol. 7, no. 1, p. 7654, 2017.
- [29] K. Mahajan, U. Garg, and M. Shabaz, "CPIDM: a clustering-based profound iterating deep learning model for HSI segmentation," *Wireless Communications and Mobile Computing*, vol. 2021, Article ID 7279260, 12 pages, 2021.